Topological spin textures in the helimagnet FeGe

M. Uchida,[1] N. Nagaosa,[2,3,4] J. P. He,[5] Y. Kaneko,[5] S. Iguchi,[3,5] Y. Matsui,[6] and Y. Tokura[2,3,4,5]
[1]*Single Quantum Dynamics Research Group, Frontier Research System (present name: Advanced Science Institute), RIKEN (The Institute of Physical and Chemical Research), Wako, Saitama 351-0198, Japan*
[2]*Cross-Correlated Materials Research Group (CMRG), ASI, RIKEN, Wako, Saitama 351-0198, Japan*
[3]*Department of Applied Physics, University of Tokyo, Tokyo 113-8656, Japan*
[4]*Correlated Electron Research Center (CERC), National Institute of Advanced Industrial Science and Technology (AIST), Tsukuba 305-8562, Japan*
[5]*Spin Superstructure Project and Multiferroics Project, ERATO, Japan Science and Technology Agency (JST), Tsukuba 305-8562, Japan*
[6]*Advanced Materials Laboratory, National Institute for Materials Science (NIMS), Tsukuba 305-0044, Japan*
(Received 1 February 2008; published 2 May 2008)

We report on the real-space observation of a type of spin texture, i.e., the Swiss-roll-like vortex, in cubic helimagnet (*B*20-type) FeGe in terms of the Lorentz electron microcopy. This structure is enabled by the weak spin anisotropy in FeGe and the two-dimensional confinement, as revealed by a theoretical analysis that takes into account the Berry phase [Proc. R. Soc. London, Ser. A **392**, 45 (1984)] associated with the curved spin stripes, i.e., the change in the spiral direction.

DOI: 10.1103/PhysRevB.77.184402 PACS number(s): 75.10.−b, 75.25.+z, 75.30.Fv

I. INTRODUCTION

Various spin textures are the subject of intensive interests both experimentally and theoretically. In this respect, helimagnets are of particular interest since the spins are destined to be noncollinear due to the frustrated exchange interactions[1,2] or the Dzyaloshinskii–Moriya (DM) interaction in noncentrosymmetric systems.[3–5] Especially, a focus of the recent intensive interests is the transition-metal silicides, such as MnSi (Refs. 6–10) and (Fe,Co)Si,[4,11] wherein the DM interaction produces spiral spin ordering with a definite helicity. In MnSi, a quantum phase transition from helimagnet to the quantum-disordered state is discovered under hydrostatic pressure at around $p_c \approx 14$ kbar.[6] A non-Fermi liquid behavior of the resistivity ρ is observed for the quantum-disordered state $p > p_c$. A neutron scattering experiment revealed the distribution of the scattering intensity on the surface of the sphere in momentum space in the quantum-disordered state.[10] This means that in MnSi, the wave vector of the spiral acts as the dynamical variable. Theoretically, several different models and/or spin textures have been proposed.[12–15] Therefore, the topological textures of helimagnets are an important problem of great current interest.

Experimental information on the spin order and texture of helimagnets is not enough yet. In our previous study,[4] the helical spin order [Fig. 1(a)] of $Fe_{0.5}Co_{05}Si$ was visualized in real space by means of the Lorentz transmission electron microscopy (TEM), in which the two types of magnetic defects, which are analogous to crystal defects, were found: the helical magnetic domain boundary and the helical magnetic edge dislocation. In the present study, we have investigated the helical spin order and the accompanying spin texture of FeGe with the *B*20 structure [Fig. 1(b)], which exhibits helical spin order with a relatively long period (70 nm) and a high Néel temperature ($T_N \sim 280$ K).[16,17] Former neutron scattering studies[16] of FeGe showed that in zero magnetic field, the helical spin propagates along the equivalent ⟨100⟩ directions between $T_N = 279$ K and T_2, where $T_{2\downarrow} = 211$ K and $T_{2\uparrow} = 245$ K in cooling and warming runs, respectively. Below T_2, however, the helical spin order changes to propagate along the equivalent ⟨111⟩ directions, implying relatively weak magnetic anisotropy. Therefore, such real-space magnetic fine structures as materializing the aforementioned topological spin texture are anticipated to show up.

II. EXPERIMENT

Single crystals of FeGe were grown by chemical vapor transport.[18] The phase purity of the crystals was checked by x-ray diffraction and magnetization measurements using a superconducting quantum interference device magnetometer.[19] The temperature dependence of the dc magnetization indicated $T_N = 280$ K, which is in accord with literature.[16,17] Thin samples for the Lorentz TEM observation were prepared by crushing the material into fine fragments with CCl_4, which were then dispersed on Cu grids coated with carbon support films. The observations were made by using a Lorentz transmission electron microscope (Hitachi HF-3000L) operated at 300 kV equipped with a television camera. The sample with perhaps a thickness of 50–100 nm was placed in a magnetic-field-free region. The Lorentz TEM has been used to observe magnetic domain in ferromagnets[20] as well as helimagnets.[4] In the wave-optical representation, the phase of an electron wave is changed as it passes through a magnetic object. Recent development of the transport of intensity equation (TIE) method allows us to obtain magnetization distributions on the basis of noninterferometric phase recovery.[21,22] The calculations were made by means of the software package QPT.[23] A detailed description of the method was given in Ref. 4.

III. EXPERIMENTAL RESULTS

The Lorentz TEM observation on many thinned crystalline fragments with different incidences revealed that the propagation vector basically prefers either of the ⟨100⟩ or the

 ©2008 The American Physical Society

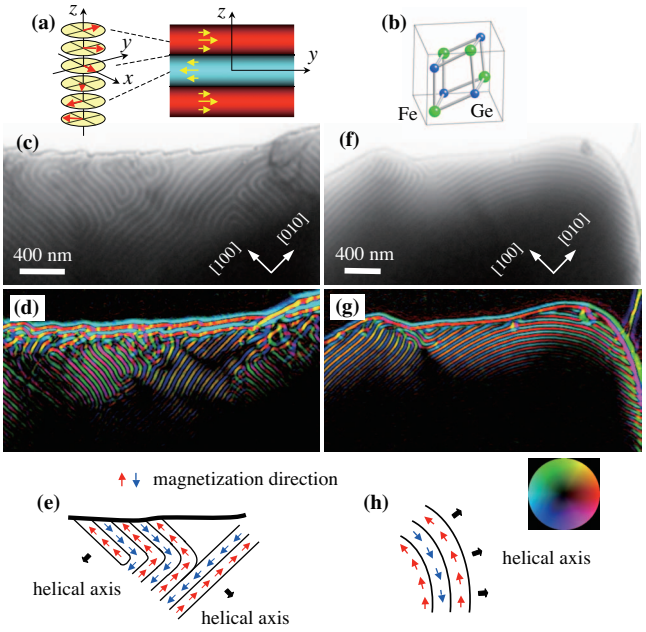

FIG. 1. (Color) Real-space observation of the helical spin order in FeGe. (a) Illustration of the helical spin order with the screw axis along the z axis in an orthogonal xyz coordinate. Spins are all parallel within one xy plane, and their direction rotates by a constant angle from one plane to a neighboring plane along the screw axis. Magnetization distribution projected on the yz plane for this helical spin order, which changes as a sinusoidal wave (Ref. 4). (b) The $B20$ crystal structure of cubic FeGe with a lattice constant of 0.470 nm. (c) An overfocused Lorentz image obtained at 200 K, which shows the magnetic twin domains arising from the helical spin order with a period of about 70 nm. The electron incidence is nearly parallel to the [001] direction. (d) A color representation of the magnetization distribution obtained by the transport of intensity equation (TIE) method, which corresponds to the state shown in (d). The direction and amplitude of the magnetization are represented by changes in color and brightness with respect to the color wheel. The contrasts on the sample edge are an artifact due to the edge effect (Fresnel fringe). (e) A schematic showing the magnetic twin domains. (f) An overfocused Lorentz image obtained at 200 K, which shows curved spin stripes. The electron incidence is nearly parallel to the [001] direction. (g) A color representation of the magnetization distribution, which corresponds to the state shown in (f). The spin stripes and the magnetizations are largely and continuously curved. (h) A schematic showing the curved spin stripe.

$\langle 111 \rangle$ direction at the temperatures between 85 K and T_N that we have studied.[3,16] However, the propagation vector does not change with temperature, which is contrary to the observation by neutron diffraction. The discrepancy between the neutron diffraction on the bulky crystal and the Lorentz TEM results arises possibly from the differences in the sample size and shape. Figure 1(c) shows an overfocused Lorentz image, which was taken at 200 K near the [001] zone axis orientation. An electron diffraction study confirmed that the observed area was a single crystallographic domain. The image clearly shows periodic stripes running either along the [100] or the [010] direction. In the focused image, the stripe patterns were confirmed to disappear, which indicate that the obtained image is magnetic in origin.[20] The magnetization distribution obtained by the TIE analysis of the overfocused and underfocused images is also shown in Fig. 1(d). A color wheel is used as a reference for the direction and amplitude of the local magnetization. The contrasts on the sample edge (the stripes running parallel along the edge) are an artifact due to the Fresnel fringe. Our analysis of the magnetization distribution revealed that the spin order is helical with a period of about 70 nm, which is in good agreement with the results determined by neutron diffraction.[16] The spin stripes cross at a right angle to each other, as schematically shown in Fig. 1(e), which is reminiscent of twin domains in crystals. The domain walls are oriented along the $\langle 100 \rangle$ direction. We note that the spin stripes appear to be connected to each other across a magnetic twin domain boundary so as to avoid discontinuities in the magnetization. In previous studies, such magnetic twin domains were postulated to explain the neutron diffraction results.[16] We were able to verify this case by the direct real-space observation.

We have also investigated the dynamics of the helimagnetic phase transition by the Lorentz TEM. The sample was gradually heated from 85 K to above T_N. The heating rate was about 2 K/min around T_N. It was difficult to determine the precise sample temperature because of the small size of the samples on the support films, but we could slowly

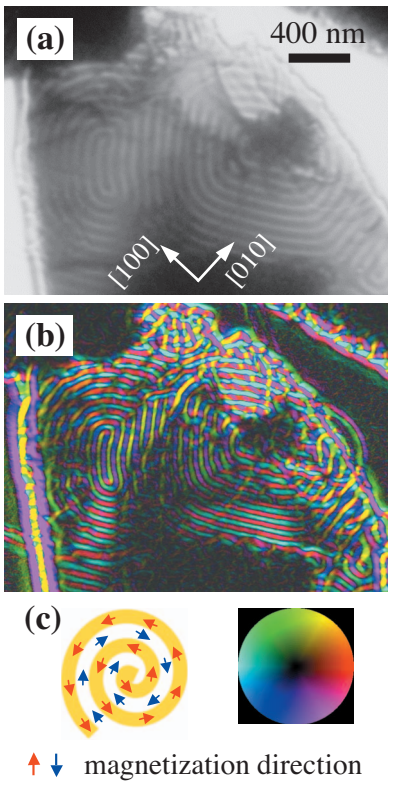

FIG. 2. (Color) Vortexlike spin stripe pattern. (a) An overfocused Lorentz image obtained at 200 K. The electron incidence is nearly parallel to the [001] direction. (b) A color representation of the magnetization distribution, which corresponds to the state shown in (a). The spin stripes arising from the helical spin order and the magnetization curl around the center. The image colors have the same meaning as in Fig. 1(d). (c) A schematic showing the Swiss-roll-like spin stripe pattern (see the text for the details). A high-resolution movie for this stripe pattern is available in Ref. 24.

traverse the helimagnetic transition temperature T_N. We observed no change in the helix period at around T_N but only the collective oscillation of the spin stripes,[24] which is the slow (second-scale) fluctuation in the phase of the stripe modulation, that was not in the amplitude. Such a collective oscillatory motion may be interpreted as a thermal phason fluctuation.[25]

Another striking feature we observed for FeGe is the existence of curved spin stripes. Figures 1(f) and 1(g) show an overfocused Lorentz image taken at 200 K near the [001] zone axis orientation and the corresponding magnetization distribution, respectively. The spin stripes as well as the magnetizations are largely and continuously curved. The curvature radius ranges from 100 to 700 nm. Such curved spin stripes indicate that the magnetic anisotropy of FeGe is small. We notice a striking difference between FeGe and $Fe_{0.5}Co_{0.5}Si$. In $Fe_{0.5}Co_{0.5}Si$, the helical magnetic domain boundary and the helical edge dislocation were observed as the major magnetic defects,[4] whereas in FeGe there are very few such magnetic defects owing to the presence of the curved spin stripes. When the temperature is increased across T_N, the similar thermal phason fluctuation to the case of the straight spin stripes was observed also for the curved spin stripes with the magnetic defects, while sometimes accompanying the annihilation of the magnetic defects in this case.

One important outcome of the curved stripes is a vortexlike spin stripe pattern. Figures 2(a) and 2(b) show an overfocused Lorentz image taken at 200 K near the [001] zone axis orientation and the corresponding magnetization distribution, respectively. The spin stripes as well as the magnetization curl show up around the center. This vortexlike spin stripe pattern is like a Swiss roll, as schematically illustrated in Fig. 2(c). The magnetization is not circularly closed and no singular point is discerned near the center of the vortex. A similar vortexlike spin stripe pattern to that shown in Fig. 2 was observed for other fragments of the specimen. It is worth noting here that a similar vortexlike pattern was observed in some chiral liquid crystals.[26] Such a Swiss-roll-like spin stripe pattern would give rise to a ringlike diffraction pattern, being reminiscent of the spheric diffraction pattern observed for the quantum-disordered helical spins of MnSi as well.[10,27,28] When the FeGe sample was heated above T_N and then cooled down to T_N, similar curved and vortexlike spin stripe patterns were reproducibly observed.

IV. THEORY FOR SPIN TEXTURES

We analyze the observed spin textures. The Hamiltonian[3] describing a helimagnet with DM interaction γ reads as

$$H = \int dr \left[\gamma \vec{M} \cdot (\nabla \times \vec{M}) + \frac{\alpha}{2} (\nabla \vec{M})^2 \right], \tag{1}$$

where α is the spin stiffness coming from the ferromagnetic exchange interaction. The ground state configuration of the magnetization $\vec{M}$ is given by

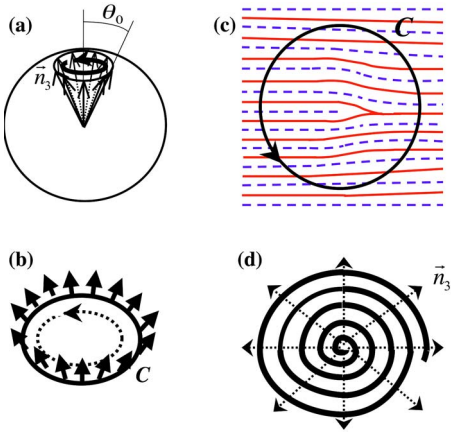

FIG. 3. (Color online) Schematic for the Berry phase (Ref. 29) and vortex structure. (a) The Berry phase (Ref. 29) associated with the change in $\vec{n}_3$ on the unit sphere with the fixed angle θ_0. (b) The change in $\vec{n}_3$ along a closed loop C in space. Here, the phason variable ψ remains constant if it is assumed to be single valued. (c) The vortex structure of ψ field as an edge dislocation of the stripe. The blue dashed (red) curves correspond to the equiphase lines with $\psi = 2\pi m$ [$\psi = (2m+1)\pi$], where m are integers. (d) The combined vortex structure of ψ and $\vec{n}_3$ fields resulting in the Swiss-roll texture.

$$\vec{M} = \frac{M}{\sqrt{2}} (\vec{n}_1 \cos \vec{Q} \cdot \vec{r} + \vec{n}_2 \sin \vec{Q} \cdot \vec{r}), \tag{2}$$

where $\vec{n}_1$ and $\vec{n}_2$ are the unit vectors orthogonal to each other, and the spiral wave vector $\vec{Q}$ is given by $\vec{Q} = (\gamma/\alpha)\vec{n}_3 \equiv (\gamma/\alpha)(\vec{n}_1 \times \vec{n}_2)$, i.e., the three vectors $\vec{n}_1$, $\vec{n}_2$, and $\vec{n}_3$ constitute the right-handed (left-handed) coordinate system for positive (negative) γ, whose directions constitute the low energy degrees of freedom. Setting Eq. (2) into Eq. (1) and keeping the lowest order term with respect to the spatial derivative assuming the slowly varying $\vec{n}_i$, we obtain the effective Hamiltonian as

$$H = \int dr \frac{\alpha M^2}{4} \{ (\nabla \vec{n}_3)^2 + 2[\nabla \psi - \nabla \varphi (1 - \cos \theta)]^2 \}. \tag{3}$$

Here, we introduce the polar coordinates as $\vec{n}_3 = (\sin \varphi \sin \theta, -\cos \varphi \sin \theta, \cos \theta)$, and the phase ψ describing the rotation of $\vec{n}_1, \vec{n}_2$ in the plane perpendicular to $\vec{n}_3$ represents the shift of the spiral along $\vec{n}_3$, i.e., phason degrees of freedom. Here, a crucial observation is that $\nabla \varphi (1 - \cos \theta)$ represents the Berry phase[29] associated with the "spin" $\vec{n}_3$. Now assume that $\vec{n}_3$ slowly changes around the north pole with θ being fixed at a small value θ_0 as one goes along a direction. Then, to minimize the energy, $\nabla \psi = \nabla \varphi (1 - \cos \theta)$ should be always satisfied, and the phase change $\Delta \psi$ of the phason that is accumulated when $\vec{n}_3$ comes back to the original direction is $\Delta \psi = \int d\vec{r} \cdot \nabla \varphi (1 - \cos \theta) = 2\pi (1 - \cos \theta_0)$, which is the solid angle subtended by the closed loop on the unit sphere drawn by $\vec{n}_3$ [Fig. 3(a)]. This means that the curved stripe leads to the phase shift of the spiral. However, when $\vec{n}_3$ changes around the loop C in the real space as shown in Fig. 3(b), the phase ψ must remain constant *if it is*

single valued. In this case, $\Delta\psi$ is zero and the energy cost from the second term in the integrand of Eq. (3) is $E_1 \approx (\alpha M^2/2)2\pi(1-\cos\theta_0)^2\log(R/a)$, where R is the radius of the sample and a is the cutoff of the order of the lattice constant. One way to reduce this logarithmically divergent energy cost is to introduce the vortex, i.e., the phase winding of $\Delta\psi$ by 2π around a core of the vortex. Figure 3(c) is the schematic view of this phason ψ vortex, wherein the lines show the loci where ψ is $2\pi m$ (blue dashed curve) and $(2m+1)\pi$ (red dashed curve), where m is an integer, and the center of the vortex corresponds to the edge dislocation of this "crystal."[4] With this vortex structure, the energy cost becomes $E_2 \approx (\alpha M^2/2)2\pi(\cos\theta_0)^2\log(R/a)+E_{\mathrm{core}}$, where E_{core} is the core energy of the vortex. Comparing E_1 and E_2, it is preferable to introduce the vortex when $\theta > \pi/3$. In the present situation, the direction of the spiral $\vec{n}_3$ is forced to lie within the xy plane, i.e., $\theta_0=\pi/2$, since the thickness of the sample in this experiment is comparable to, or thinner than, the period of the spiral. Therefore, the logarithmic energy cost in E_2 vanishes, although the first term in the integrand of Eq. (3) still gives the logarithmically divergent energy cost as in the case of usual vortex. The Swiss-roll structure is schematically shown in Fig. 3(d), wherein the vortex structures of the phason ψ and $\vec{n}_3$ are combined. Therefore, we conclude that this spin texture is stabilized by the coupling between the phason ψ and the spiral direction $\vec{n}_3$ through the geometrical Berry phase.[29] The present spin texture should exhibit a higher free energy than that of the simple helical spin structure.[3] However, the presence of the thermodynamically metastable spin texture is similar to the case of the dislocation in crystal; such a spin texture must be induced by the boundary condition of the specimen shape or the nonadiabatic cooling procedure. Once this structure is realized, however, it is topologically stable according to the following homotopy classification. The order parameter space of helimagnets is SO(3) and its fundamental group is $\pi_1[\mathrm{SO}(3)] = Z_2$,[30] and, hence, there is only one type of topological vortex. However, when the direction $\vec{n}_3$ is confined within the xy plane, the order parameter space becomes $\mathrm{U}(1)\times\mathrm{U}(1)$, as described above. Also, the magnetic anisotropy, which prefers some directions of $\vec{n}_3$, gives the energy cost of the $\vec{n}_3$ vortex. This can be written as the term $h\cos 4\varphi$ in the Hamiltonian, and the energy of the vortex becomes proportional to the linear size of the sample, which is similar to the case of a domain wall. However, the argument for the logarithmic energy increase in the second term of Eq. (3) remains true and the Swiss-role structure is more stable than the simple $\vec{n}_3$ vortex. When h is too large, on the other hand, the vortex structure itself is suppressed and we believe that this is the reason why it was not observed in (Fe, Co)Si.[4]

V. CONCLUSION

We have reported the real-space observation of the helical spin order of cubic FeGe by means of the Lorentz TEM. We could directly image the magnetic twin domains in the single crystallographic domain as well as the curved spin stripes with the change in the spiral direction, the most notable of which is the Swiss-roll-like stripe vortex. A theoretical account for these spin textures are given, which shows that the vortex structure is stabilized due to the Berry phase[29] associated with the curved spin stripes. In addition, we have reported on the real-space dynamics of the helimagnetic phase transition, in which the observed collective oscillatory motion was interpreted as a thermal phason fluctuation.

ACKNOWLEDGMENTS

Valuable discussions with C. Pfleiderer and T. Senthil are greatly acknowledged. One of the authors (N.N.) acknowledges support from a Grant-in-Aid (No. 19048015) from MEXT, Japan.

[1] A. Yoshimori, J. Phys. Soc. Jpn. **14**, 807 (1959).
[2] Y. Tokura, Science **312**, 1481 (2006).
[3] P. Bak and M. H. Jensen, J. Phys. C **13**, L881 (1980).
[4] M. Uchida, Y. Onose, Y. Matsui, and Y. Tokura, Science **311**, 359 (2006).
[5] M. Bode, M. Heide, K. von Bergmann, P. Ferriani, S. Heinze, G. Bihlmayer, A. Kubetzka, O. Pietzsch, S. Blügel, and R. Wiesendanger, Nature (London) **447**, 190 (2007).
[6] C. Pfleiderer, S. R. Julian, and G. G. Lonzarich, Nature (London) **414**, 427 (2001).
[7] N. Doiron-Leyraud, I. R. Waker, L. Taillefer, M. J. Steiner, S. R. Julian, and G. G. Lonzarich, Nature (London) **425**, 595 (2003).
[8] W. Yu, F. Zamborszky, J. D. Thompson, J. L. Sarrao, M. E. Torelli, Z. Fisk, and S. E. Brown, Phys. Rev. Lett. **92**, 086403 (2004).
[9] Y. J. Uemura, T. Goko, I. M. Gat-Malureanu, J. P. Carlo, P. L. Russo, A. T. Savici, A. Aczel, G. J. MacDougall, J. A. Rodriguez, G. M. Luke, S. R. Dunsiger, A. McCollam, J. Arai, C. Pfleiderer, P. Böni, K. Yoshimura, E. Baggio-Saitovitch, M. B. Fontes, J. Larrea, Y. V. Sushko, and J. Sereni, Nat. Phys. **3**, 29 (2007).
[10] C. Pfleiderer, D. Reznik, L. Pintschovius, H. V. Löhneysen, M. Garst, and A. Rosch, Nature (London) **427**, 227 (2004).
[11] Y. Onose, N. Takeshita, C. Terakura, H. Takagi, and Y. Tokura, Phys. Rev. B **72**, 224431 (2005).
[12] U. K. Rößler, A. N. Bogdanov, and C. Pfleiderer, Nature (London) **442**, 797 (2006).
[13] B. Binz, A. Vishwanath, and V. Aji, Phys. Rev. Lett. **96**, 207202 (2006).
[14] S. Tewari, D. Belitz, and T. R. Kirkpatrick, Phys. Rev. Lett. **96**, 047207 (2006).
[15] J. Schmalian and M. Turlakov, Phys. Rev. Lett. **93**, 036405 (2004).
[16] B. Lebech, J. Bernhard, and T. Freltoft, J. Phys.: Condens. Matter **1**, 6105 (1989).
[17] P. Pedrazzini, H. Wilhelm, D. Jaccard, T. Jarlborg, M. Schmidt, M. Hanfland, L. Akselrud, H. Q. Yuan, U. Schwarz, Yu. Grin, and F. Steglich, Phys. Rev. Lett. **98**, 047204 (2007).

[18] M. Richardson, Acta Chem. Scand. (1947-1973) **21**, 2305 (1967).
[19] M. Uchida (unpublished).
[20] A. Hubert and R. Schäfer, *Magnetic Domains* (Springer, New York, 1998).
[21] S. Bajt, A. Barty, K. A. Nugent, M. McCarney, M. Wall, and D. Paganin, Ultramicroscopy **83**, 67 (2000).
[22] M. Uchida, R. Mahendiran, Y. Tomioka, Y. Matsui, K. Ishizuka, and Y. Tokura, Appl. Phys. Lett. **86**, 131913 (2005).
[23] *QPt, Version 1.0* (HREM, Saitama, Japan, 2004).
[24] See EPAPS Document No. E-PRBMDO-77-059814 for the movies. A direct link to this document may be found in the online article's HTML reference section. The document may also be reached via the EPAPS homepage (http://www.aip.org/pubservs/epaps.html) or from ftp.aip.org in the directory/epaps/. See the EPAPS homepage for more information.
[25] G. Grüner, Rev. Mod. Phys. **66**, 1 (1994).
[26] H. Goto and K. Akagi, Macromolecules **25**, 1482 (2004).
[27] Y. Ishikawa and M. Arai, J. Phys. Soc. Jpn. **53**, 2726 (1984).
[28] S. V. Grigoriev, S. V. Maleyev, A. I. Okorokov, Yu. O. Chetverikov, R. Georgii, P. Böni, D. Lamago, H. Eckerlebe, and K. Pranzas, Phys. Rev. B **72**, 134420 (2005).
[29] M. V. Berry, Proc. R. Soc. London, Ser. A **392**, 45 (1984).
[30] D. Mermin, Rev. Mod. Phys. **51**, 591 (1979).